Available online at www.sciencedirect.com
ScienceDirect
Journal of Power Sources 163 (2006) 598–603
JOURNAL OF POWER SOURCES
www.elsevier.com/locate/jpowsour

Short communication

Role of TiB_2 and Bi_2O_3 additives on the rechargeability of MnO_2 in alkaline cells

V. Raghuveer, A. Manthiram *

Materials Science and Engineering Program, The University of Texas at Austin, Austin, TX 78712, USA

Received 30 July 2006; received in revised form 24 August 2006; accepted 15 September 2006
Available online 27 October 2006

Abstract

With an aim to understand the role of recently reported Ti-containing additives like TiB_2 on the rechargeability of manganese oxide cathodes in alkaline cells, a redox reaction involving the chemical oxidation of $Mn(OH)_2$ with H_2O_2 in KOH solution and a non-redox reaction involving the reaction of Mn(III) acetate with KOH have been carried out in the presence and absence of 1 wt% TiB_2 and 0.5 wt% TiB_2 + 4.5 wt% Bi_2O_3 additives. The solid products formed during the reactions have been analyzed by X-ray diffraction and a redox titration to determine the oxidation state of manganese while the filtrate has been analyzed to determine the amount of dissolved manganese with reaction time. The results suggest that irreversible reactions that follow the disproportionation reaction of dissolved Mn^{3+}, which leads to the formation of electrochemically inactive phases like birnessite (δ-MnO_2) and hausmannite (Mn_3O_4) and a consequent decline in capacity retention, are suppressed in the presence of the TiB_2 additive, with the suppression being more effective when Bi_2O_3 is present along with TiB_2.

Keywords: Rechargeable alkaline batteries; Manganese oxide cathode; Chemical additives; Reaction mechanisms

1. Introduction

Rechargeable batteries based on electrolytic manganese dioxide (EMD) cathodes are attractive as manganese is abundant, inexpensive, and environmentally benign. EMD, which is referred to as γ-MnO_2, has a tunnel structure formed by an intergrowth of pyrolusite (β-MnO_2) and ramsdellite domains. However, the commercialization of rechargeable alkaline cells has been hampered by the poor rechargeability of EMD cathodes. Kordesch et al. [1–3] made significant progress and devised a rechargeable manganese dioxide (RAM^{TM}) cell involving one electron per manganese. The one-electron transfer process involves discharging γ-MnO_2 to δ-MnOOH by proton intercalation into the tunnels [4–7]. Although the one-electron process is reversible to some extent at lower depth of discharge (<0.5 e/Mn), a slow but steady capacity fade was found to occur at deep discharge (>0.5 e/Mn) that limits the service life of the cells [1–8].

Interestingly, incorporation of Bi- and Ba-containing additives into EMD has been found to enhance the rechargeability considerably [8–13]. Our group [14–17] showed from an X-ray diffraction analysis of the cycled manganese oxide cathodes in the one-electron regime that the formation of electrochemically inactive phases such as birnessite (δ-MnO_2) and hausmannite (Mn_3O_4) is partly responsible for the capacity fade. With a number of chemical reaction experiments to simulate the electrochemical reactions, our group also showed that the formation of the unwanted electrochemically inactive phases is due to the chemical instability of the discharged form (δ-MnOOH) of EMD [16]. The dissolution from the lattice and subsequent disproportionation of the Mn^{3+} ions are responsible for the formation of unwanted birnessite and hausmannite phases. The incorporation of Bi- or Ba-containing compounds into the cathode delays the disproportionation reaction of Mn^{3+} by keeping the Mn^{3+} ions in solution for longer time and thereby suppresses the formation of the electrochemically inactive phases.

Recently, we reported that Ti-containing additives such as TiB_2 improves the cyclability of EMD significantly [18] compared to the previously known Bi_2O_3 additive. Structural characterization with X-ray diffraction of the cycled electrodes and an analysis of the manganese redox process with slow-scan

* Corresponding author. Tel.: +1 512 471 1791; fax: +1 512 471 7681.
E-mail address: rmanth@mail.utexas.edu (A. Manthiram).

0378-7753/$ – see front matter © 2006 Elsevier B.V. All rights reserved.
doi:10.1016/j.jpowsour.2006.09.029

cyclic voltammetry revealed that the better cyclability in the presence of TiB_2 is due to a suppression of the formation of the electrochemically inactive phases (birnessite and hausmannite) and a shifting of the second-electron capacity of Mn to higher potentials. With an aim to understand the role of Ti-containing additives in suppressing the formation of the electrochemically inactive phases and compare the results with those of the previously known Bi_2O_3 additive, we present here the results of some designed chemical reaction experiments that simulate the electrochemical reactions. Specifically, the oxidation reactions of $Mn(OH)_2$ with H_2O_2 in KOH solution (a redox reaction) and the reaction of Mn(III) acetate with KOH (a non-redox reaction) in the presence and absence of three additive compositions (1 wt% TiB_2, 0.5 wt% TiB_2 + 4.5 wt% Bi_2O_3, or 5 wt% Bi_2O_3), followed by an analysis of the solid and filtrate are presented.

2. Experimental

2.1. Materials

Electrolytic manganese dioxide was supplied by Chemmetals, Inc. Manganese(II) acetate tetrahydrate (99%, Acros Organic), manganese(III) acetate dihydrate (Alfa Aesar), titanium boride (Alfa Aesar), potassium hydroxide (99%, Fisher), and Bi_2O_3 (Alfa Aesar) were used as received. All other chemicals were purchased from commercial sources and were used without further purification.

2.2. Electrochemical measurements

Thin film type electrodes of about 5–8 mg weight were prepared by mixing the modified EMD (75 wt%) consisting of small amounts of the additives (1 wt% TiB_2, 0.5 wt% TiB_2 + 4.5 wt% Bi_2O_3, or 5 wt% Bi_2O_3) with graphite (Timrex SFG-15, 20 wt%), and polytetrafluoroethylene (PTFE) binder (5 wt%) in a mortar and pestle, followed by rolling into thin sheets. The thin film electrode was then mounted onto a nickel mesh current collector. The discharge/charge measurements were carried out with a three-electrode assembly using Hg/HgO (in 9 M KOH) as reference electrode, a porous nickel counter electrode consisting of $NiOOH/Ni(OH)_2$, and 9 M KOH as the aqueous electrolyte. The cycling experiments were carried out under constant current discharge/charge conditions between −0.4 and +0.35 V versus Hg/HgO with discharge and charge rates of, respectively, *C*/2 and *C*/4, with no rest period between discharge and charge measurements.

2.3. Chemical oxidation and non-redox reactions

The chemical oxidation reactions (redox reaction) of $Mn(OH)_2$ with H_2O_2 were carried out as follows: 1.23 g of manganese(II) acetate tetrahydrate was dissolved in 70 mL of deionized water. 0.0123 g of TiB_2 (in the case of 1 wt% TiB_2 additive) or 0.0062 g of TiB_2 + 0.0554 g of Bi_2O_3 (in the case of 0.5 wt% TiB_2 + 4.5 wt% Bi_2O_3 additive) was then dispersed into the manganese(II) acetate solution thus prepared. The $Mn(OH)_2$ suspension in 7 M KOH was generated by adding an appropriate amount of KOH pellets into the above solution within 15 s. To the suspension, 0.283 g of H_2O_2 was added in order to get the final average oxidation state of manganese to be +3, and the mixture was stirred with a magnetic stirrer. After a specific length of time, the solid was filtered, washed thoroughly, dried, and analyzed by X-ray diffraction. The oxidation state of manganese in the solid was analyzed with a redox titration employing the sodium oxalate method. The amount of Mn in the filtrate was determined by atomic absorption spectroscopy after diluting a fixed volume (2 mL) of filtrate to 100 mL and carrying out the measurement within 30 min of filtration to suppress any error arising from further precipitation.

The experiments with the non-redox type reactions were also carried out in a manner similar to that described in the previous paragraph. First, 0.2 g of manganese(III) acetate and 0.002 g of TiB_2 (in the case of 1 wt% TiB_2 additive) or 0.001 g of TiB_2 + 0.009 g of Bi_2O_3 (in the case of 0.5 wt% TiB_2 + 4.5 wt% Bi_2O_3 additive) were dispersed in 70 mL of deionized water. Then, an appropriate amount of KOH pellets were added to make the solution to have a net concentration of 7 M KOH. After a specific length of time, the solid and filtrate were separated and analyzed as described in the previous paragraph.

3. Results and discussion

3.1. Cyclability

The effect of various amounts of TiB_2 additive on the cyclability of EMD has been reported elsewhere [18]. Fig. 1 compares the cyclabilities of the EMD cathodes in the presence and absence of 0.5 wt% TiB_2, 1 wt% TiB_2, 5 wt% Bi_2O_3, and 0.5 wt% TiB_2 + 4.5 wt% Bi_2O_3 in the one-electron regime. Both the additions of TiB_2 alone and Bi_2O_3 alone improve the cyclability compared to plain EMD, but the combined addition of 0.5 wt% TiB_2 and 4.5 wt% Bi_2O_3 provides the best cyclability among the different additives presented in Fig. 1.

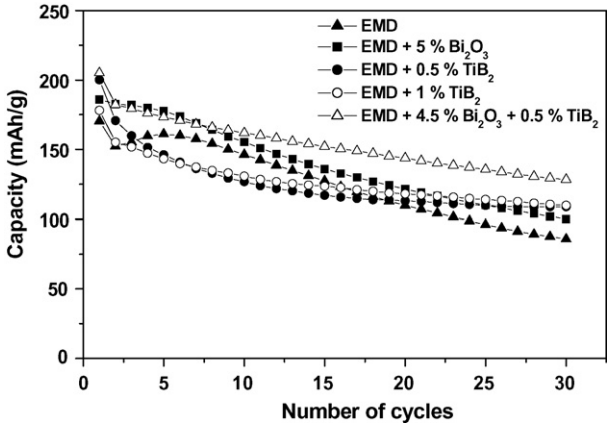

Fig. 1. Comparison of the cyclability of EMD in the absence and presence of TiB_2, Bi_2O_3, and TiB_2 + Bi_2O_3 additives. The capacity values are per gram of the active material MnO_2.

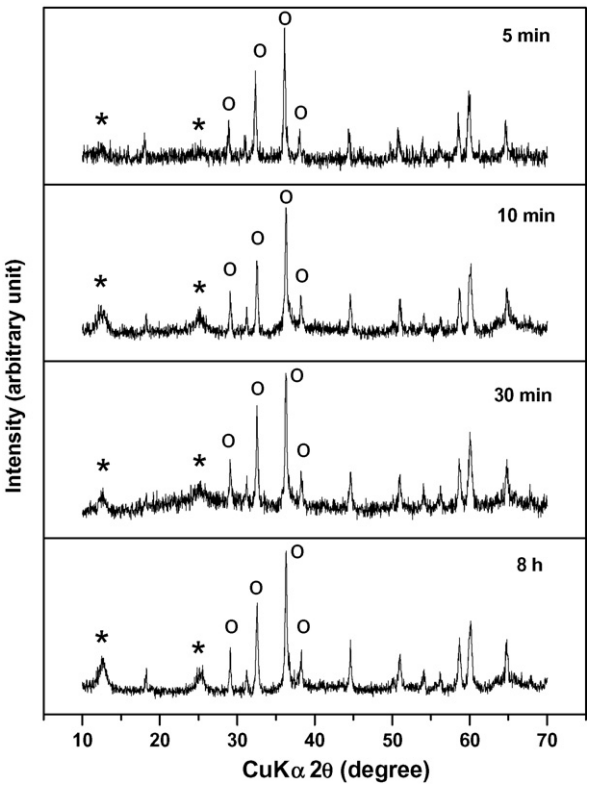

Fig. 2. Evolution with reaction time of the X-ray diffraction patterns of the solid products obtained by oxidizing $Mn(OH)_2$ with H_2O_2 in 7 M KOH without any additives. The reflections marked with * and ◯ refer, respectively, to birnessite (δ-MnO_2) and hausmannite (Mn_3O_4) phases.

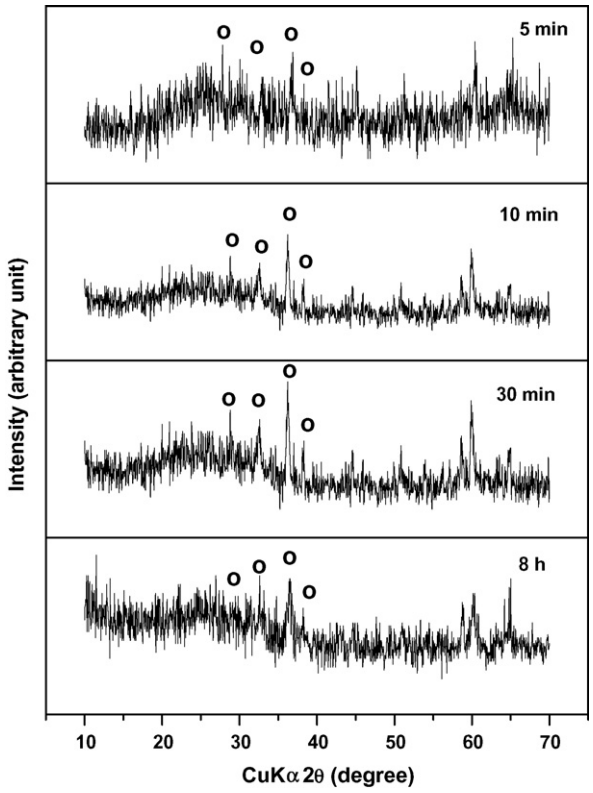

Fig. 3. Evolution with reaction time of the X-ray diffraction patterns of the solid products obtained by oxidizing $Mn(OH)_2$ with H_2O_2 in 7 M KOH with 1 wt% TiB_2 additive. The reflections marked with ◯ refer to hausmannite (Mn_3O_4).

3.2. Chemical oxidation reaction with H_2O_2

The color of the reaction mixture turned into black on adding H_2O_2 to the $Mn(OH)_2$ suspension in KOH that was prepared as described in Section 2, indicating the oxidation of Mn^{2+} into Mn^{3+}. Figs. 2–4 compare the X-ray diffraction patterns of the solid products obtained in the absence (Fig. 2) and presence of 1 wt% TiB_2 (Fig. 3) and 0.5 wt% TiB_2 + 4.5 wt% Bi_2O_3 (Fig. 4) additives. In the absence of additives, well-defined reflections corresponding to birnessite and hausmannite are readily developed within a short reaction time of as low as 5 min (Fig. 2). With increasing reaction time, no significant changes in the X-ray patterns are observed up to 8 h excepting a gradual growth of the birnessite reflections, indicating aging [19,20]. On the other hand, in the presence of 1 wt% TiB_2 additive, the X-ray diffraction patterns are not well defined even after 8 h of reaction time (Fig. 3), possibly due to the effect of TiB_2 in preventing the formation of well crystalline manganese oxide phases. However, weak reflections corresponding to the hausmannite phase could be seen even after 5 min, which grow with further increase in reaction time. In the presence of a mixture of 0.5 wt% TiB_2 and 4.5 wt% Bi_2O_3 (Fig. 4), a broad reflection observed around $2\theta = 19^\circ$ might correspond to those of $Mn(OH)_2$ and β-MnOOH. This is similar to that found with the electrochemical oxidation of $Mn(OH)_2$, in which β-MnOOH is a transitional oxidation product. Interestingly, the reflections corresponding to the hausmannite phase are much weaker in the case of 0.5 wt% TiB_2 + 4.5 wt% Bi_2O_3 additive compared to that in the presence of 1 wt% TiB_2 additive. Moreover, no reflections corresponding to birnessite are observed even after 8 h in the case of both 1 wt% TiB_2 and 0.5 wt% TiB_2 + 4.5 wt% Bi_2O_3 additives. These results reveal that both TiB_2 and Bi_2O_3 are effective in suppressing the formation of the unwanted, electrochemically inactive phases, but the mixture of TiB_2 and Bi_2O_3 is more effective than the individual TiB_2 or Bi_2O_3 additives.

The variations of the average oxidation state of manganese in the solid products with reaction time are shown in Fig. 5. In the absence of additives, the average oxidation state of manganese during the initial stages of the reaction remains close to +3.0. On the other hand, oxidation state values greater than +3.0 are found in the presence of both 1 wt% TiB_2 additive and 0.5 wt% TiB_2 + 4.5 wt% Bi_2O_3 additive. These observations are similar to those found before with the Bi- and Ba-containing additives [16]. The constancy of the oxidation state with time in the absence of additive could be due to the formation of stable phases such as birnessite and hausmannite at the early stages of the reaction, while the increase in oxidation state with time could be due to the aerial oxidation of manganese hydroxide with time. These observations are consistent with the X-ray data in Figs. 2–4.

Fig. 6 compares the variations in the concentration of manganese in the filtrate with reaction time. In the absence of additives, the concentration of manganese in the filtrate is low, indicating a quick formation of solid phases as expected from

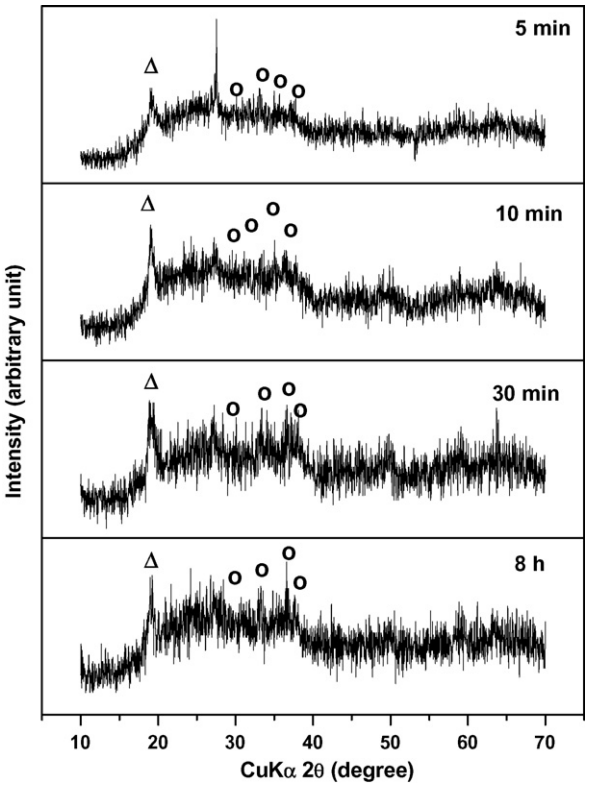

Fig. 4. Evolution with reaction time of the X-ray diffraction patterns of the solid products obtained by oxidizing $Mn(OH)_2$ with H_2O_2 in 7 M KOH with 0.5 wt% TiB_2 + 4.5 wt% Bi_2O_3 additive. The reflections marked with Δ and ◯ refer, respectively, to $Mn(OH)_2$ or β-MnOOH and hausmannite (Mn_3O_4).

the X-ray diffraction data in Fig. 2. In the presence of additives, the concentration of manganese in the filtrate is higher compared to that in the absence of additives, but the difference is larger in the presence of 0.5% TiB_2 + 4.5% Bi_2O_3 additive than that in the presence of 1 wt% TiB_2 additive. The results suggest that the additives are effective in preventing the dissolved species

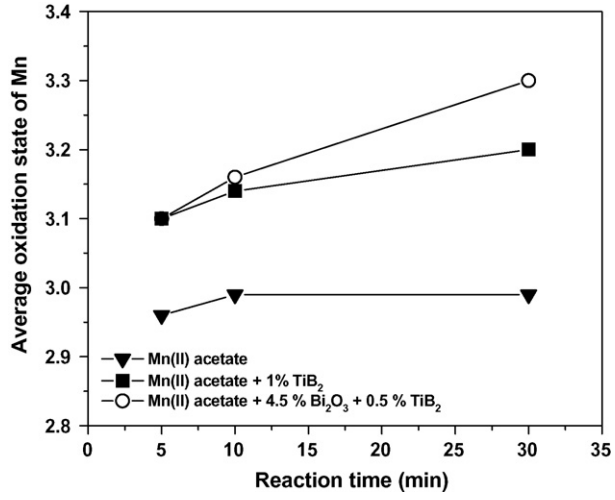

Fig. 5. Variations with reaction time of the average oxidation state of manganese in the solid product obtained by oxidizing $Mn(OH)_2$ with H_2O_2 in 7 M KOH solution in the absence and presence of additives.

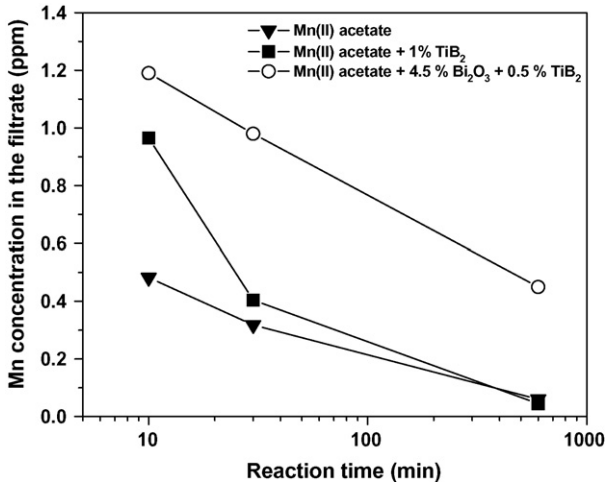

Fig. 6. Variations with reaction time of the concentration of manganese in the filtrate obtained by oxidizing $Mn(OH)_2$ with H_2O_2 in 7 M KOH solution in the absence and presence of additives.

from forming solid phases, but the mixture of TiB_2 and Bi_2O_3 is much more effective than individual TiB_2. It is known that Mn^{2+} has a tendency to stay in solution, and higher concentration of manganese may mean more Mn^{2+} species in solution. Thus, one would expect more Mn^{4+} ions in the solid to account for the total charge, which is in accordance with the oxidation state data in Fig. 5. The decrease in the concentration of manganese with time in Fig. 6 is partially due to an aerial oxidation to give Mn^{4+} in the solid as indicated by the increase in manganese valence in the solid in Fig. 5.

3.3. Non-redox reaction in KOH

The results in the previous section indicate that the dissolved manganese ions have a tendency to form solid phases and the rate of such reactions could be delayed by the incorporation of additives like TiB_2 into the reaction medium, which is similar to the observation made with Bi- and Ba-containing additives before by our group [16]. With the chemical oxidation method, only the total number of electron change can be controlled with some Mn^{3+} being oxidized further to Mn^{4+} on reacting with H_2O_2 while some Mn^{2+} remain unchanged because of the concentration depletion of the oxidizing agent. With an aim to investigate the stability of Mn^{3+} species in the absence of oxidizing agents, we carried out a non-redox reaction, in which a well-known Mn^{3+} salt, manganese(III) acetate, was employed as the starting material. The addition of KOH to Mn(III) acetate would generate $[Mn(OH)_6]^{3-}$ complex, and any detection of Mn^{2+} or Mn^{4+} would confirm the occurrence of the disproportionation reaction of Mn^{3+} to Mn^{4+} and Mn^{2+}. Figs. 7 and 8 compare, respectively, the variations of the average oxidation state of manganese in the solid and the concentration of manganese in the filtrate. Although the magnitude of the values are different from those obtained with the oxidation reaction with H_2O_2, the trends observed in Figs. 7 and 8 are similar to those in Figs. 5 and 6, validating the discussion in the previous section.

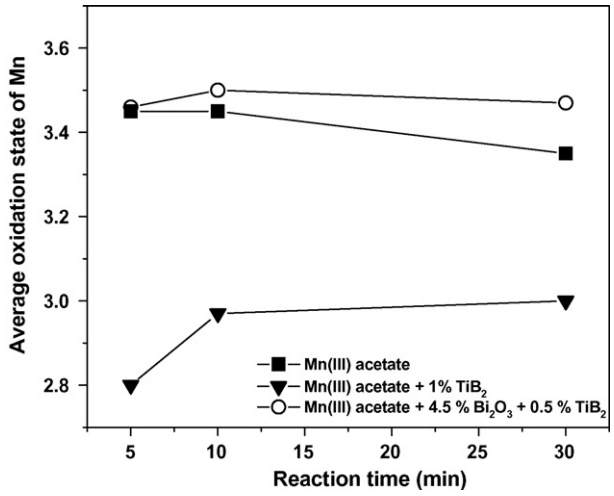

Fig. 7. Variations with reaction time of the average oxidation state of manganese in the solid product obtained by reacting manganese(III) acetate with 7 M KOH solution in the absence and presence of additives.

3.4. Role of TiB_2 and $TiB_2 + Bi_2O_3$ additives on the cyclability of γ-MnO_2

Based on our results in the previous sections and some earlier studies in the literature [6,13,15,21], the reaction mechanism suggested by our group before [16] for the formation of birnessite and hausmannite phases with the Bi- and Ba-containing additives could also be applicable in the case of the TiB_2 additive as discussed below. The pertinent reactions are:

Dissolution of Mn^{3+} from oxides or oxyhydroxides in alkaline medium

$$MnOOH \leftrightarrow [Mn(OH)_6]^{3-} \quad (1)$$

Disproportionation of Mn^{3+} ions in solution

$$[Mn(OH)_6]^{3-} \leftrightarrow [Mn(OH)_6]^{4-} + [MnO_2]^{\#} \quad (2)$$

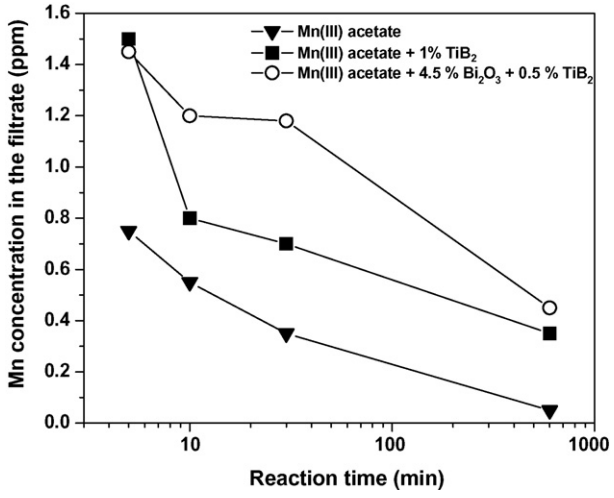

Fig. 8. Variations with reaction time of the concentration of manganese in the filtrate obtained by reacting manganese(III) acetate with 7 M KOH solution in the absence and presence of additives.

Irreversible formation of birnessite from Mn^{4+} containing solid

$$[MnO_2]^{\#} \rightarrow \delta\text{-}MnO_2 \quad (3)$$

Irreversible formation of hausmannite by the reaction between Mn^{2+} and Mn^{3+} complexes

$$2[Mn(OH)_6]^{3-} + [Mn(OH)_6]^{4-} \rightarrow Mn_3O_4 \quad (4)$$

It is known that Mn^{3+} ions are soluble in strongly alkaline solution to some extent by forming a Mn^{3+} complex as shown in reaction (1). Hence, a solid containing Mn^{3+} would be in equilibrium with Mn^{3+} complex in the solution and the solubility will be determined by the solubility product, which in turn depends on the differences in the Gibbs free energies between the solid phase and the complex ion. Earlier studies indicate that manganese ions are dissolved out from the reduced γ-MnO_2 in alkaline solutions. The detection of manganese ions in the filtrate solution irrespective of the additives suggests that the TiB_2 additives do not prevent the dissolution of Mn^{3+} from the solid, which is similar to that found before with the Bi- and Ba-containing additives [16]. The $[MnO_2]^{\#}$, which is an en route to birnessite formation (reaction (3)), is the transitional oxide with short-range order or small crystallite size that is produced immediately after the disproportionation reaction (2). The absence of reflections corresponding to Mn^{4+} oxides in the X-ray diffraction pattern (Figs. 3 and 4) and average oxidation state greater than +3 (Figs. 5 and 7) in the presence of TiB_2 or $TiB_2 + Bi_2O_3$ additive confirm the formation of transitional oxides.

However, the immediate formation of birnessite (Fig. 2) and the increase in the intensity of its reflection around $2\theta = 12^\circ$ without an increase in the oxidation state (Figs. 5 and 7) in the absence of additives seem to suggest that the rate of formation of birnessite from the transitional oxide, $[MnO_2]^{\#}$, is quite rapid in the absence of additives. While the increase in the average oxidation state with reaction time in the presence of 1 wt% TiB_2 and 0.5% $TiB_2 + 4.5\%$ Bi_2O_3 additives (Figs. 5 and 7) suggests that the additives affect the formation reactions of birnessite (reaction (3)) and hausmannite (reaction (4)) rather than the disproportionation reaction (2). The absence of reflections corresponding to birnessite in Figs. 3 and 4 indicates the effective suppression of the irreversible reaction (3) by the TiB_2 and $TiB_2 + Bi_2O_3$ additives. It is well known that hausmannite is formed irreversibly through a solution path (reaction (4)) because of its high chemical stability. The weak reflections corresponding to hausmannite in the presence of the $TiB_2 + Bi_2O_3$ additive (Fig. 4) compared to that in the presence of individual TiB_2 additive (Fig. 3) indicate that the irreversible hausmannite formation reaction (4) is being suppressed effectively by the mixture of TiB_2 and Bi_2O_3. The results thus indicate that TiB_2 with and without Bi_2O_3 effectively suppresses the reaction that leads to the formation of electrochemically inactive phases (birnessite and hausmannite) rather than the disproportionation reaction, which is consistent with the improved cyclability data in Fig. 1. However, further work is essential to understand the nature of the species or complexes formed by the interaction of Mn with Ti in the absence and presence of Bi that is responsible for the enhanced cyclability of the EMD cathodes.

4. Conclusions

The incorporation of a small amount (0.5–1 wt%) of TiB_2 with and without Bi_2O_3 into EMD improves the cyclability of EMD in the one-electron regime after an initial drop in capacity between the first and second cycles compared to that found with the previously known additive Bi_2O_3. The enhanced cyclability is due to the suppression of the formation of unwanted, electrochemically inactive birnessite and hausmannite phases [18]. Results of some designed redox and non-redox chemical reactions indicate that the incorporation of TiB_2 additives with and without Bi_2O_3 helps to keep the manganese ions in solution for a longer time, thereby suppressing the irreversible formation of stable phases such as birnessite and hausmannite, with $TiB_2 + Bi_2O_3$ being more effective than TiB_2 alone. Optimization of the amount of additives could further improve the cyclability of manganese oxides and have an impact on the commercialization feasibility of rechargeable alkaline cells based on manganese oxide cathodes.

Acknowledgment

Financial support by the Texas Higher Education Coordinating Board (Technology Development and Transfer grant 003658-0582-2003) and RBC Technologies is gratefully acknowledged.

References

[1] K. Kordesch, J. Gsellmann, M. Peri, K. Tomantschger, R. Chemelli, Electrochim. Acta 26 (1981) 1495.
[2] K. Kordesch, M. Weissenbacher, J. Power Sources 51 (1994) 6.
[3] Y.W. Shen, K. Kordesch, J. Power Sources 87 (2000) 162.
[4] A. Kozawa, R.A. Powers, J. Electrochem. Soc. 113 (1966) 870.
[5] Y. Chabre, J. Pannetier, Prog. Solid State Chem. 23 (1995) 1.
[6] C. Mondoloni, M. Laborde, J. Rioux, E. Andoni, C. Levy-Clement, J. Electrochem. Soc. 139 (1992) 954.
[7] D. Boden, C.J. Venuto, D. Wisler, R.B. Wylie, J. Electrochem. Soc. 114 (1967) 415.
[8] Y.F. Yao, N. Gupta, H.S. Wroblowa, J. Electroanal. Chem. 223 (1987) 107.
[9] M.A. Dzieciuch, N. Gupta, H.S. Wroblowa, J. Electrochem. Soc. 135 (1988) 2415.
[10] H.S. Wroblowa, N. Gupta, J. Electroanal. Chem. 238 (1987) 98.
[11] C.G. Castledine, B.E. Conway, J. Appl. Electrochem. 25 (1995) 707.
[12] S.W. Donne, G.A. Lawrance, D.A.J. Swinkels, J. Electrochem. Soc. 144 (1997) 2961.
[13] N. Bode, C. Cachet, S. Bereira-Ramos, J.C. Ginoux, L.T. Yu, J. Electrochem. Soc. 144 (1997) 792.
[14] A.M. Kannan, S. Bhavaraju, F. Prado, M. Manivel Raja, A. Manthiram, J. Electrochem. Soc. 149 (2002) A483.
[15] D. Im, A. Manthiram, J. Electrochem. Soc. 150 (2003) A68.
[16] D. Im, A. Manthiram, B. Coffey, J. Electrochem. Soc. 150 (2003) A1651.
[17] V. Raghuveer, A. Manthiram, Electrochem. Commun. 7 (2005) 1329.
[18] V. Raghuveer, A. Manthiram, J. Power Sources 59 (2006) 1468.
[19] J. Luo, Q. Zhang, S.L. Suib, Inorg. Chem. 39 (2000) 741.
[20] Y. Ma, L. Luo, S.L. Suib, Chem. Mater. 11 (1999) 1972.
[21] D.Y. Qu, B.E. Conway, L. Bai, Y.H. Zhou, W.A. Adams, J. Appl. Electrochem. 23 (1993) 693.